Preparation of PDMS−PMAA Interpenetrating Polymer Network Membranes Using the Monomer Immersion Method

J. S. Turner and Y.-L. Cheng*

Department of Chemical Engineering and Applied Chemistry, University of Toronto, Toronto, Ontario M5S 3E5, Canada

Received November 5, 1999; Revised Manuscript Received January 29, 2000

ABSTRACT: A monomer immersion sequential method for preparing PDMS−PMAA interpenetrating polymer networks (IPNs) was developed. Immersion of pre-IPN films in the guest monomer throughout synthesis ensured an even monomer concentration profile and produced a uniform bicontinuous morphology throughout the IPN indicative of phase separation by spinodal decomposition. Such IPNs were permeable to water-soluble compounds. Laser scanning confocal microscopy (LSCM) of the swollen IPNs allowed direct visualization of the morphology. PDMS−PMAA sequential IPNs synthesized while in contact with surfaces were also examined. Contact with glass or air during synthesis resulted in spatially varying morphology ranging from dispersed hydrogel domains near the surface to a bicontinuous morphology some distance below the surface. The morphology spectrum was attributed to a monomer concentration gradient created by monomer evaporation during handling of the pre-IPN film, as well as to substrate-dependent surface thermodynamic effects. The layer near the surface with dispersed hydrogel domains rendered such IPN membranes impermeable to water-soluble compounds.

Introduction

An interpenetrating polymer network (IPN) has been described as an intimate entanglement of two cross-linked networks.[1] It is believed that the interlocked structure of the cross-linked components ensures the stability of the bulk and surface morphologies and makes IPNs superior to other types of multicomponent structures.[2,3] Rubber-hydrogel IPNs may also bring unique advantages to some biomaterial and drug delivery applications due to their bicontinuous morphologies and relatively small hydrogel domain sizes (10−200 nm). Continuity in the permeable phase is necessary for drug delivery applications, while bicontinuity is required for applications such as contact lens materials, where transport of oxygen and water occurs in different phases. The relative size of the guest polymer phase is also an important consideration for the mechanical strength and mass transfer properties of IPNs. Because of the simultaneous polymerization and cross-linking that occurs during preparation, phase separation does not reach thermodynamic equilibrium. Cross-linking renders any entanglements permanent.[3] These factors allow for the formation of small domains in otherwise incompatible polymer mixtures.

The bicontinuous nature and hydrogel domain size of IPNs are dependent to a large extent on the mechanism by which the two component polymers phase separate during IPN formation. Phase separation of multicomponent polymer systems can occur by either nucleation and growth (NG) which leads to a morphology of isolated guest polymer domains dispersed within the host polymer network (sea−island morphology) or spinodal decomposition (SD) which produces a bicontinuous structure of relatively small, interconnected nodular domains of the guest polymer in the host polymer network.[4]

* Corresponding author: Tel 1-416-978-5500; FAX 1-416-978-8605; e-mail ylc@chem-eng.utoronto.ca.

Work by Sperling[1] and Kim[5] has shown that for sequential IPNs phase separation mechanisms are highly dependent on the composition of the guest polymer in the IPN network. In a more recent study,[6] a morphology spectrum created along the thickness direction of the membrane was attributed to the different phase separation mechanisms taking place as a result of an intentionally created guest monomer concentration gradient. At low guest monomer concentrations, a sea−island morphology was formed via NG. As guest monomer concentration increased, a dual morphology was observed where both sea−island and interconnected nodular morphologies had formed by both NG and SD, respectively. As guest monomer concentration increased further, phase separation occurred via only SD, producing a nodular interconnected guest polymer phase. Aside from these studies, very little research has focused on the effect of IPN preparation method or the IPN−substrate interface on the distribution of monomer in the pre-IPN film and the resultant IPN morphology.

Gradient morphology formation and surface enrichment have been examined to a greater extent for blends[7−9] and copolymers.[10] For these systems, it has long been known that the surface compositon is different from the bulk and that surface segregation is significantly affected by the interfacial energy at the polymer−substrate interface. The polymer component which minimizes the interfacial energy will segregate to the surface. The formation of a gradient morphology in the surface region is a direct consequence of the surface segregation of the one polymer.

Preparation of rubber-hydrogel IPNs has involved placing the IPN against a surface of either Teflon,[2,11,12] Mylar,[13] or glass[14,15] without explicitly controlling monomer distribution in the pre-IPN films. Surface segregation of the rubber component was found in some studies. He et al.[15] placed a polysiloxane/acrylic acid monomer mixture onto a glass sheet to form an IPN. They found that the surface consisted of a 5 nm layer of siloxane and that the surface wettability was very low. Mura-

10.1021/ma991873k CCC: $19.00
Published on Web 04/27/2000

yama et al.[2] prepared IPNs from poly(2-hydroxyethyl methacrylate) (PHEMA) and polystyrene (PS) using the sequential method by placing the pre-IPN films onto Teflon. XPS studies found that the PS component was enriched in the surface of the IPN and that a gradient composition of the two polymers existed in the first 100 μm of the surface region. The gradient composition at the surface was attributed to the inhibition of styrene polymerization due to O_2 diffusing into the IPN, as well as the effects of surface thermodynamic at the IPN−substrate interface during polymerization.

The morphology at and adjacent to the surface may affect both the biocompatibility and mass transfer properties of an IPN and is therefore crucial to the use of IPNs in biomaterial and drug delivery applications. In this study, we examined the effect of the IPN−substrate interface and IPN preparation method on the morphology of rubber-hydrogel IPNs. Specifically, IPNs of poly(dimethylsiloxane) and poly(methacrylic acid) were prepared using glass, air, or pure methacrylic acid monomer as the contacting surface. The morphology of the resulting IPNs was characterized using laser scanning confocal microscopy (LSCM), and the existence or absence of a bicontinuous morphology was further corroborated via permeation studies. The use of pure methacrylic acid monomer as the contacting medium during IPN preparation—the "monomer immersion method"—is a novel method of IPN synthesis developed in this work to produce IPNs with bicontinuous morphologies. The bicontinuous morphologies are produced directly as a result of the homogeneous distribution of monomer in the pre-IPN film.

Experimental Section

Materials. The materials used to prepare the PDMS host polymer network were vinyl-terminated PDMS (65 000 cst), platinum−divinyltetramethyldisiloxane (United Chemical Technologies, Bristol, PA), and a cyclic hydride-containing cross-linking agent (MDX4-4210, Dow Corning, Midland, MI). The PMAA guest polymer network was prepared from methacrylic acid and triethylene glycol dimethacrylate (Polysciences Inc., Warrington, PA) and 2,2-dimethoxyacetophenone (Irgacure 651, Ciba Geigy), a UV-sensitive free radical initiator. Citrate and phosphate buffer solutions were prepared from citric acid monohydrate, sodium citrate, sodium hydrogen phosphate, sodium dihydrogen orthophosphate, and sodium azide (Sigma Chemical Co.). Vitamin B_{12} (MW 1355, Sigma Chemical Co.) was used as the permeant for permeation studies. Fluorescein (sodium salt) was used as the hydrophilic fluorescent agent for LSCM studies.

Preparation of PDMS Film. Poly(dimethylsiloxane) (PDMS) resin (116 000 Da, 65 000 cst) containing 60 ppm of platinum divinyltetramethyldisiloxane complex and 4% MDX4-4210, a cyclic, multifunctional silicone hydride cross-linker, was spread to a thickness of approximately 0.5 μm on a Mylar sheet using polyethylene (PE) spacers. The resin was then placed under a vacuum of 25 mmHg for approximately 6 h in order to remove any entrapped air bubbles within the bulk of the film. This was followed by a hydrosilyation addition at 55 °C for 24 h. The cured PDMS resin was die cut into circular sections with diameters of 20 mm.

Each circular PDMS section was placed in cyclohexane with mixing for 24 h in order to wash away any unreacted PDMS components. The degree of swelling in cyclohexane was also used to determine the molecular weight between cross-links of the PDMS polymer network.

Preparation of PDMS−PMAA IPN. Monomer Immersion Method. The washed PDMS sections were then immersed in methacrylic acid monomer solution containing 1% w/v of 2,2-dimethoxyacetophenone, the UV-sensitive free radical initiator, and 1% v/v of triethylene glycol dimethacrylate, the cross-linker for approximately 18 h. The swollen PDMS network (pre-IPN film) contained approximately 50% MAA monomer. The pre-IPN film was purged with N_2, then immersed in MAA monomer without cross-linking agent or photoinitiator, and placed under UV light having an intensity of 32 W and a wavelength of 350 nm for 1 h. The resultant IPN, a hard, tough crystalline material, was washed extensively in distilled water to remove any unreacted component and to reach equilibrium swelling. Once completely washed, the IPN contained approximately 30% PMAA on a dry basis.

Air−IPN Interface Method. The circular PDMS sections were placed in methacrylic acid monomer solution as outlined above. Using a glovebox, the pre-IPN film was purged with N_2 and transferred to an empty scintillation vial. The film was placed against the wall of the glass vial so that one surface contacts the glass wall and the other forms a free surface. The vial was capped and placed under UV irradiation and subsequently washed as detailed above.

Glass−IPN Interface Method. Within a glovebox, the pre-IPN film (prepared as above) was transferred to a square cover glass slide. The film was surrounded by a PE spacer which was held in place using silicone grease, and then a second cover glass slide was placed on top of the film. The pre-IPN film was essentially sandwiched between the two glass slides and then placed under UV irradiation for 1 h and subsequently washed as detailed above.

LSCM of IPN Morphology. Although LSCM has been used to examine the morphology of blends, there are no examples in the literature where it has been used for IPNs, possibly because IPN domain sizes are usually much smaller than LSCM resolution (100−200 nm). In this work, we show that, by examining PDMS−PMAA IPNs in their swollen state (pH 7), the hydrogel domains are sufficiently large that LSCM visualization of the morphology is possible.

LSCM studies were carried out using an inverted microscope, the Carl Zeiss LSM 510 using a 488 nm argon laser. Two-dimensional optical sections at different depths along the optical axis of the microscope (z direction) were taken with a water-immersible ×63 objective lens (N.A. = 1.2). The size of the images obtained in the $x-y$ plane was 29.2 μm × 29.2 μm. The image was captured with a resolution of 512 pixels × 512 pixels and 8 bit gray scale depth. Resolution along the z axis was 0.65 μm. The spatial resolution was approximately 244 nm. Images were taken at the surface and at corresponding planes below the surface at 1 μm intervals.

Use of a fluorescent marker (fluorescein sodium salt) to distinguish the hydrogel domains from the rubbery network allowed for sharp image contrast between the rubber and hydrogel regions. The white regions in the LSCM images represent PMAA hydrogels domains that were were accessible to fluorescein when IPN films were placed in fluorescein solution, i.e., those that were connected to the external surfaces, including the faces as well as the circumferential surfaces, of the IPNs. The black regions represent fluorescein-free portions of the IPNs, either PDMS or isolated PMAA hydrogel domains which were inaccessible to fluorescein. The images were further analyzed using Corel PhotoPaint to obtain percent fluorescent area as a function of depth for each IPN−interface system. All pixels in a bitmap image above a certain red tonal value (threshold value = 41) were defined as being fluorescent. Since fluorescent areas represent the accessible gel regions in the membrane, these figures allowed us to assess the relative accessible gel regions as a function of depth in a semiquantitative fashion. The results were not used to compare the different IPNs since fluorescent intensity was highly dependent on LSCM parameters and membrane conditions at the time of image capture.

Swelling Studies and Permeation Studies. Swelling studies were carried out for PDMS−PMAA IPN membranes in phosphate buffer of pH 7. Equilibrium swollen mass and dry mass were used to calculate the hydration of the IPN at pH 7, defined as the mass fraction of water in the swollen IPN. Permeation studies were carried out at 37 °C using standard two compartment diffusion cells. The donor chamber was filled with the permeant (vitamin B_{12}) dissolved in a buffer solution of specified pH, and the receptor chamber was filled with the

same buffer containing no permeant. The receptor chamber was sampled at specified time intervals. The volume removed was replaced with fresh buffer. Approximate infinite sink condition was maintained in all experiments. The sample solutions were monitored at 362 nm for vitamin B_{12} using a Hewlett-Packard 8450 UV−vis spectrophotometer.

Results and Discussion

PDMS−PMAA IPNs were prepared using the sequential method where the monomer-swollen pre-IPN film was placed against a glass substrate (glass-IPN), interfaced with air (air−IPN), or immersed in the pure monomer of the IPN's guest polymer (monomer−IPN), during guest monomer polymerization and cure. At pH 7, all three materials had an equilibrium hydration value of approximately 0.84. Despite the high hydration, no permeation of vitamin B_{12} through the air−IPN and glass−IPN membranes could be detected over a 1 month permeation experiment. This corresponds to a value of permeability of less than 1.9×10^{-13} cm^2/s. In contrast, the permeability of VB12 through the monomer−IPN membrane was found to be 6.5×10^{-8} cm^2/s at pH 7. The morphology of these materials was further examined using a laser scanning confocal microscope (LSCM) in order to understand why some materials of significant hydration were not permeable to water-soluble compounds and to determine the effect of substrate and preparation methods on the bicontinuous morphology of the IPN—particularly in the surface and subsurface regions. We hypothesized that both the IPN−substrate interface and the mode of IPN preparation had a significant effect on the guest monomer concentration profile at the surface and subsurface regions, which in turn affected the morphology in each IPN system. LSCM images for the three types of IPNs are shown in black and white in Figures 1−3 with white representing the fluorescent regions, while the percent fluorescence area vs depth for each IPN is shown in Figure 4.

Glass−IPN Interface. Parts a−f of Figure 1 are optical sections of an IPN prepared against a glass surface, a substrate known to thermodynamically favor contact with hydrophilic polymers and ionic monomers. An image taken at the surface (Figure 1a) shows large (0.5−2 μm) irregular PMAA hydrogel domains. Images taken between 1 and 12 μm below the surface were all black (Figure 1b), implying either that no hydrogel domains were present or that any hydrogel domains which might be present were encapsulated in PDMS and inaccessible to fluorescein. The latter scenario is typical of a dispersed sea−island morphology formed by the NG phase separation mechanism and is indicative of low monomer concentrations in the pre-IPN film. Kim et al.[6] were able to visualize such a morphology using SEM because their guest polymer domains were significantly larger in the dry state (1 μm diameter) than those in this study. On the basis of the results of Kim and images taken of layers above and below the 14 μm fluorescent-free area, a plausible argument can be made that dispersed hydrogel domains existed in this area due to the low monomer concentration created during the evaporation of monomer prior to placing against the glass substrate and due to migration of the monomer to the glass−substrate interface. A layer with such a morphology would be impermeable to water-soluble compounds such as fluorescein and vitamin B_{12}. At a depth of 14 μm, spherical, connected hydrogel domains of approximately 3−5 μm in diameter were visible (Figure 1c). From 14 to 18 μm in depth (Figure 1d) the

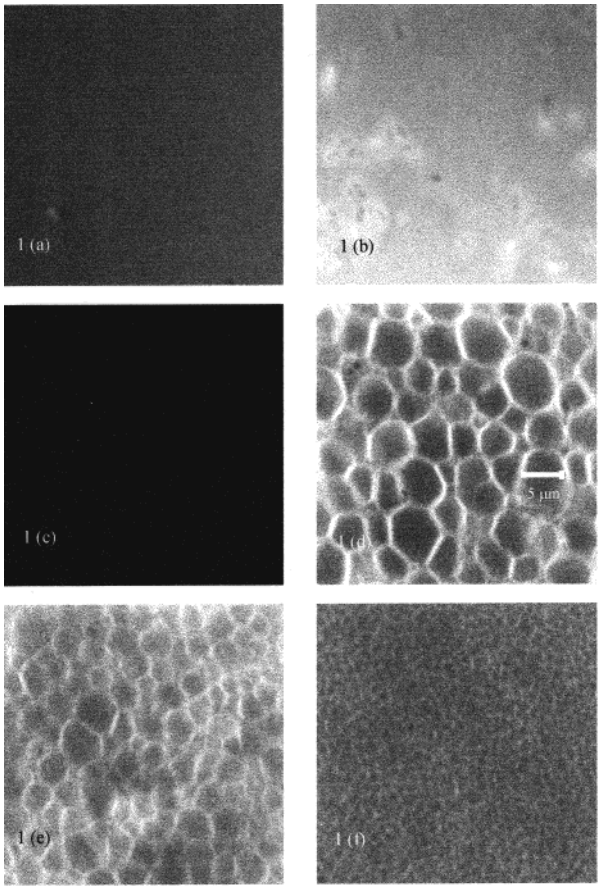

Figure 1. LSCM images of depth profile of IPN prepared with a glass substrate (glass−IPN): (a) surface, (b) 2 μm, (c) 14 μm, (d) 18 μm, (e) 24 μm, and (f) 30 μm.

spherical hydrogel domains increased in concentration. At 24 μm (Figure 1e), spherical domains were still visible; however, the presence of small nodular domains within the spheres became evident. This region of dual phase morphology, where large dispersed spheres have begun to connect forming a bicontinuous, permeable structure due to the phase separation taking place by both SD and NG, is clearly evident in the LSCM images. This region represents a transition in mechanisms of phase separation and is consistent with a higher monomer concentration than the surface layer. At 30 μm (Figure 1f) only small, nodular gel domain morphology was present, and this morphology continued to a depth of about 60 μm. Monomer concentration had increased so that only SD occurred at this depth. LSCM detection further into the IPN was not possible.

It should be noted that other than the first 5 μm near the surface, the morphology spectrum just described was seen in all glass−IPN films examined. The morphology at the surface varied with lateral position and ranged from isolated gel domains to uniform gel layers up to 5 μm in thickness. The enrichment of hydrogel at the surface is consistent with the hydrophilic nature of the glass surface. The nonuniformity of the surface layer can be attributed to uneven contact between the pre-IPN film and glass and evaporation of the MAA monomer prior to placing against the glass substrate.

Figure 4a quantitatively shows the percent fluorescent area versus depth for the glass−IPN based on the series of images shown in Figure 1. The most striking feature of Figures 1 and 4a was the 14 μm fluorescent-free layer adjacent to the surface of the glass−IPN. The

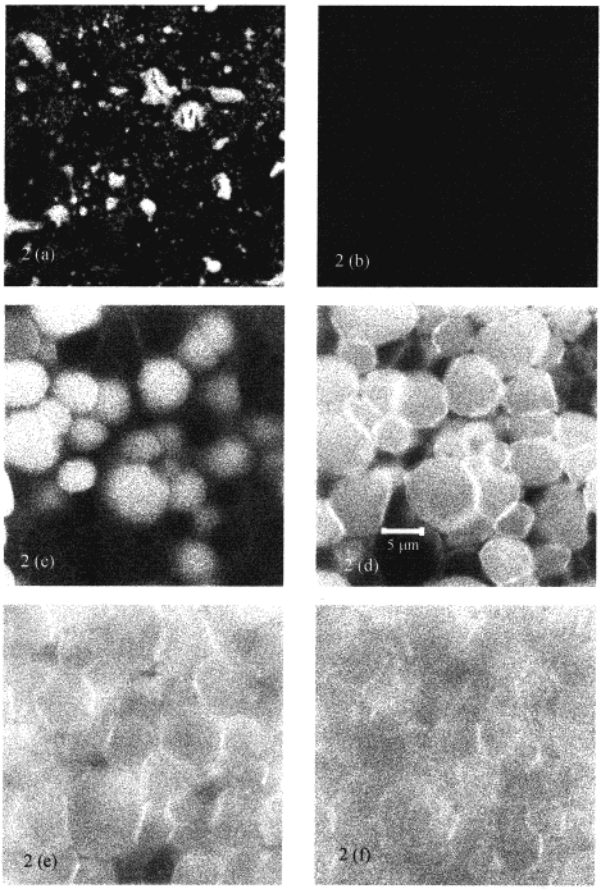

Figure 2. LSCM images of depth profile of IPN prepared with a free surface (air−IPN): (a) surface, (b) 5 μm, (c) 10 μm, (d) 40 μm, (e) 50 μm, and (f) 60 μm.

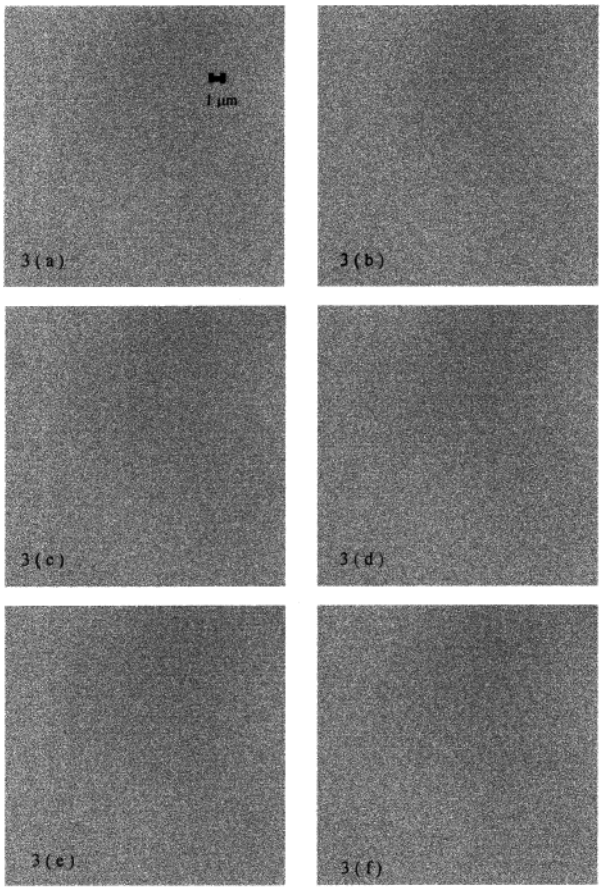

Figure 3. LSCM images of depth profile of IPN prepared using monomer immersion method: (a) surface, (b) 10 μm, (c) 20 μm, (d) 30 μm, (e) 40 μm, and (f) 50 μm.

pattern of morphology shown in these images was similar to the morphology spectrum described by Kim[6] and was attributed to the monomer concentration gradient produced due to evaporation while placing the pre-IPN film onto the glass substrate and migration of monomer to the IPN−glass substrate.

Air−IPN Interface. Parts a−f of Figure 2 are optical sections of an IPN prepared with an air−IPN interface (air−IPN). At the surface of the air−IPN (Figure 2a) there is a PDMS-enriched layer with some nodular gel domains (0.7% fluorescent area compared to the overall hydration of 0.84, Figure 4b). Similar nodular gel domains are also visible at 5 μm below the surface (Figure 2b), but at a higher concentration (98% fluorescent area, Figure 4b). From 10 to 30 μm (Figure 2c) the LSCM images were black, indicating the absence of accessible PMAA hydrogel regions. The existence of a black subsurface layer can be attributed to the same monomer evaporation mechanism and redistribution of monomer in the surface region due to surface thermodynamics at the air−IPN interface.

It was expected that at the air−IPN interface a surface layer of PDMS would exist due its low surface energy; however, the large increase in hydrogel at 5 μm was unexpected. The enclosed nitrogen envrionment in which the polymerization and cross-linking of the IPN took place was most likely saturated with monomer vapor from the pre-IPN film, and this may have affected the final hydrogel composition of the surface layer. A mass balance calculation based on the vapor pressue of MAA at room temperature and the composition of gel at the air−IPN surface supports this explanation.

Proceeding inward from the black layer, the morphology at 40 μm (Figure 2d) changed to large spheres of PDMS-rich domains surrounded by PMAA-rich boundaries to give a honeycomb-like appearance. A similar morphology was seen at 50 μm (Figure 2e); however, the PMAA-rich boundaries appeared to be more diffuse, and within each honeycomb, small, nodular PMAA-rich domains were visible. This honeycomb appearance for the hydrogel component was different than the large gel spheres observed in the region of dual phase morphology for the glass−IPN membrane. In this membrane, it was the PDMS-rich regions which have formed spheres. This structure may possibly be due to a phase inversion which has taken place during IPN formation. At 60 μm (Figure 2f) no evidence of spheres or honeycomb-like structures could be seen; the separate phases had a nodular shape typical of SD. This morphology continued up to 100 μm below the surface, at which point LSCM detection was no longer possible.

Monomer−IPN Interface. Figure 3a−f shows the LSCM images of a monomer−IPN starting at the surface of the IPN and progressing into the bulk of the IPN to a depth of 50 μm. There was a slightly lower concentration of PMAA regions at the surface of the IPN (Figures 3a and 4c). This was attributed to the diffusional release of cross-linking agent and initiator from the pre-IPN film when it was placed in pure MAA monomer prior to UV irradiation. The diffusional release would slow considerably as polymerization and cross-linking progressed, thus isolating MAA depletion to only near the surface.

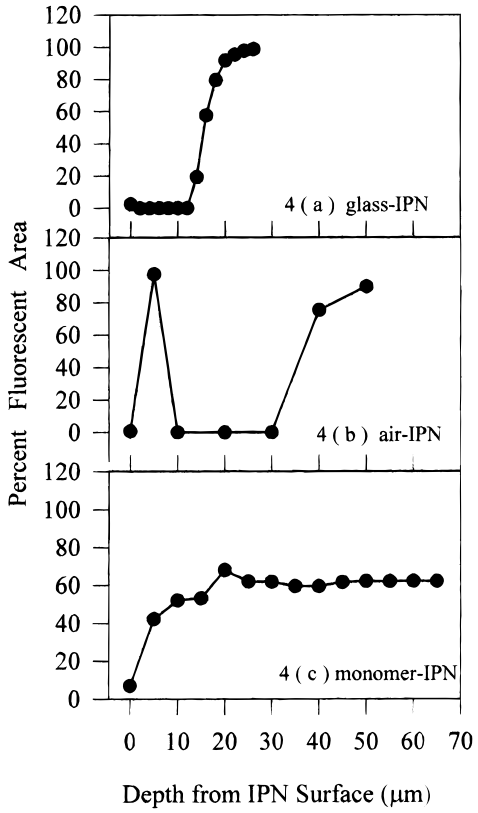

Figure 4. Percent fluorescent area as a function of depth from IPN surface for LSCM images of (a) glass−IPN, (b) air−IPN, and (c) monomer−IPN.

The qualitative morphological features of the PDMS−PMAA IPN prepared by the monomer immersion method were similar throughout the IPN. The IPN consisted of uniformly dispersed hydrogel domains (approximately 100−200 nm in dimension) within the host PDMS network. The morphology was characteristic of bicontinuous structures formed by SD. Figure 4c illustrates the uniform concentration of accessible hydrogel domains as a function of gel depth produced by the monomer immersion method.

The monomer immersion method of IPN preparation was developed in this work to overcome the problem of nonuniform morphologies created due to the formation of a monomer concentration gradient when conventional modes of IPN preparation−formation of the IPN against a substrate[2,11,13−15] (glass−IPN) or as a free surface (air−IPN) were used. It was hypothesized that the gradient morphology spectrum formed in these membranes was due to a poorly controlled monomer composition in the pre-IPN film. Monomer concentration profiles could be created either due to evaporation during IPN preparation or as a result of surface segregation at the IPN−substrate interface. By surrounding the pre-IPN film with guest monomer during IPN formation, a uniform distribution of MAA in the pre-IPN film was maintained while polymerization and cross-linking of MAA took place resulting in a uniform, bicontinuous morphology throughout the membrane thickness.

In this work, the monomer immersion method was developed for an IPN system in which the guest monomer could diffuse into the host polymer without requiring a cosolvent. In less compatible systems that require a cosolvent, the same method can be applied simply by carrying out guest monomer polymerization and cross-linking while immersing the pre-IPN in a solution of the monomer in the cosolvent.

Conclusions. The effect that different substrates, as well as method of preparation, have on the surface morphology of the rubber-hydrogel IPN material was examined. IPNs prepared against a glass substrate or as a free surface produced a morphology spectrum ranging from dispersed hydrogel domains near the surface to a dual phase morphology, followed by a bicontinuous morphology indicative of spinodal decomposition. This morphology spectrum created an impermeable layer near the surface of the membrane, rendering even highly, hydrated membranes impermeable to water-soluble compounds. The formation of the impermeable layer was attributed to the evaporation of monomer during the casting of the pre-IPN film, as well as the redistribution of monomer at the IPN−substrate interface which was dependent on the particular substrate used during synthesis.

The monomer immersion method of IPN preparation produced bicontinuous rubber-hydrogel IPN membranes with phase morphology indicative of spinodal decomposition. This allowed for high hydration values and permeability to water-soluble solutes at pH 7 conditions. The monomer immersion method minimized the monomer concentration gradient in the pre-IPN film caused by either evaporation or surface thermodynamics and produced a uniform, bicontinuous morphology throughout the membrane thickness.

References and Notes

(1) Sperling, L. H.; Mishra, V. In *IPNs Around the World*; Kim, S. C., Sperling, L. H., Eds.; John Wiley & Sons Ltd.: New York, 1997; p 1.
(2) Murayama, S.; Kuroda, S. *Polymer* **1993**, *34*, 3845−3852.
(3) Suthar, B.; Xiao, H. X.; Klempner, D.; Frisch, K. C. In *IPN's Around the World*; Kim, S. C., Sperling, L. H., Eds.; John Wiley & Sons Ltd.: New York, 1997; p 49.
(4) (a)Strobl, G. R. *The Physics of Polymers: Concepts for Understanding Their Structures and Behaviour;* Springer: Berlin, 1996. (b) Park, J. W.; Kim, S. C. In *IPNs Around the World*; Kim, S. C., Sperling, L. H., Eds.; John Wiley & Sons Ltd.: New York, 1997; p 27.
(5) Kim, Y.; Kim, S. *Macromolecules* **1999**, *32*, 2334−2341.
(6) Xie, X.; Chen, Y.; Zhang, Z.; Tanioka, A.; Matsuoka, M.; Takemura, K. *Macromolecules* **1999**, *32*, 4424−4429.
(7) Chen, Z.; Ward, R.; Tian, Y.; Eppler, A. S.; Shen, Y. R.; Somorjai, G. *J. Phys. Chem. B* **1999**, *103*, 2935−2942.
(8) Zhang, D.; Gracias, D. H.; Ward, R.; Gauckler, M.; Tian, Y.; Shen, Y. R.; Somorjai, G. *J. Phys. Chem. B* **1998**, *102*, 6225−6230.
(9) Senshu, K.; Furuzono, T.; Koshizaki, N.; Yamashita, S.; Matsumoto, T.; Kishida, A.; Akashi, M. *Macromolecules* **1997**, *30*, 4421−4428.
(10) McGarey, B.; McLenaghan, D. W.; Richards, R. W. *Br. Polym. J.* **1989**, *21*, 227−232.
(11) Murayama, S.; Kuroda, S.; Osawa, Z. *Polymer* **1993**, *34*, 3893−3898.
(12) Bae, Y. H.; Okano, T.; Kim, S. W. U.S. Patent 4,931,287, 1999.
(13) Ingenito, D. R.; Rugge, H. F.; Soane, D. S.; Sturm, W. L. U.S. Patent 5,789,483, 1998.
(14) He, X.; Herz, J.; Meyer, G.; Widmaier, J. U.S. Patent 5,424,-375, 1995.

MA991873K